Trading off Charging and Sensing for Stochastic Events Monitoring in WRSNs

Yu Sun*†, Chi Lin*†‡, Haipeng Dai‡§, Qiang Lin¶, Lei Wang*†, and Guowei Wu*†‖
*School of Software Technology, Dalian University of Technology, Dalian 116023, China
†Key Laboratory for Ubiquitous Network and Service Software of Liaoning Province, Dalian 116621, China
‡State Key Laboratory for Novel Software Technology, Nanjing University, Nanjing, Jiangsu 210024, China
§Jiangsu High Technology Research Key Laboratory for Wireless Sensor Networks, Nanjing, Jiangsu 210003, China
¶Dalian University of Science and Technology, Dalian 116052, China
‖Acoustics Science and Technology Laboratory, Harbin Engineering University, Harbin 150001, China
Email: yusun.dut@gmail.com, {c.lin, wgwdut}@dlut.edu.cn, haipengdai@nju.edu.cn, lqchina@126.com, lei.wang@ieee.org

***Abstract*—As an epoch-making technology, wireless power transfer incredibly achieves energy transmission wirelessly, enabling reliable energy supplement for wireless rechargeable sensor networks (WRSNs). Existing methods mainly concentrate on performance improvement theoretically, neglecting the fact that most Commercial Off-The-Shelf (COTS) rechargeable sensors (*e.g.*, WISP and Powercast) are not allowed to conduct sensing and energy harvesting tasks simultaneously, termed *charging exclusivity*. Therefore, their schemes are not feasible for practical applications. In this paper, we focus on the charging exclusivity issue in stochastic events monitoring while improving network performance. In specific, we pay close attention to trading off charging and sensing tasks and formulate a combinatorial optimization problem with routing constraints. We introduce novel discretization techniques and investigate the routing problem to reformulate the original problem into the maximization of a submodular function. With a slightly relaxed budget, the output of our proposed algorithm is better than $(1-1/e)/2$ of the optimal solution to the original problem with a smaller charging radius $(1-\xi)D_c$. Through extensive simulations, numerical results show that in terms of charging utility, our algorithm outperforms baseline algorithms by 21.3% on average. Moreover, we conduct test-bed experiments to demonstrate the feasibility of our scheme in real scenarios.**

I. Introduction

Wireless power transfer technology [1] has provided effective means for energy replenishment in Wireless Rechargeable Sensor Networks (WRSNs) [2]–[6], in which sensors are with rechargeable batteries to harvest energy through wireless signals transmitted by wireless charging vehicles (WCVs).

In recent years, much effort has been devoted to charging performance optimizations in WRSNs [7], [8], such as: maximizing charging utility [9], minimizing charging time [10], network lifetime extension [11], and so on. In these works, they assume that energy harvesting and event sensing can be simultaneously conducted by sensors. However, this assumption contradicts practical applications to some extent, especially for COTS (Commercial Off-The-Shelf) wireless charging equipment. In this kind of equipment (*e.g.*, Powercast [12] and WISP [13]), energy capture modules and onboard supercapacitors are implemented instead of traditional lithium batteries for efficient energy harvesting. However, COTS rechargeable sensors are lightweight and simple in structure, which lacks complex power control circuits [12]. As a result, the onboard supercapacitor is confined to one of the two statuses: charging or discharging. Thereby, simultaneous charging and sensing cannot be achieved. State-of-the-art methods [14], [15] emphasized the feasibility of theoretical results/analysis. However, in realistic scenarios, their schemes do not perform well based on aforementioned COTS devices. This critical issue motivates us to propose a scheme that is not only suitable for theoretical results/analysis, but also feasible in practical applications.

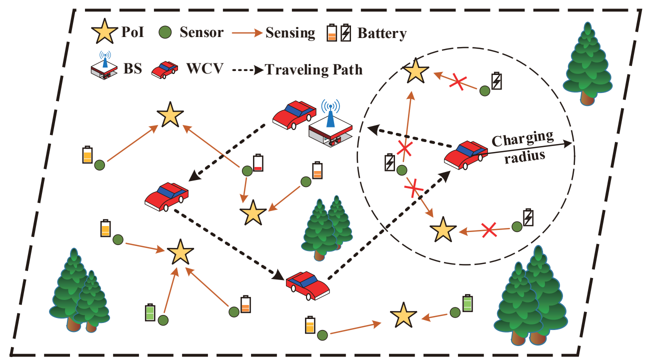

Fig. 1. Network model.

In our network scenario (as shown in Figure 1), when a sensor is being charged, the sensing behavior will be suspended until the charging process ends, which indicates that *charging and sensing cannot co-exist simultaneously on a COTS rechargeable sensor*, which is called *charging exclusivity phenomenon*. If the charging exclusivity issue is not appropriately resolved, some critical events will be missed, leading to catastrophic consequences, which is extremely prohibited especially in real-time and safety-critical applications, such as health caring [16]. In this paper, we focus on how to effectively improve the charging utility (see definition in Section III-B) while introducing the effect of *charging exclusivity*.

Specifically, we form a practical monitoring model for stochastic events in which each sensor has a specific monitoring

Chi Lin*†‡ is the corresponding author.

978-1-7281-6992-7/20/$31.00 © 2020 IEEE

probability for each Point of Interest (PoI) within its sensing range. On this basis, we present a practical event model and a utility model which takes charging exclusivity into account and propose the Charging Exclusivity Optimization (CEO) problem. We try to select appropriate sojourn spots for a single WCV to charge surrounding sensors such that the charging utility under the influence of charging exclusivity is maximized, while ensuring that the energy cost of WCV will not exceed its budget.

However, when solving the CEO problem, we are confronting with several critical challenges:

- First, the charging exclusivity problem may lead to incidental utility loss when WCV conducts charging tasks. It is non-trivial to quantitatively leverage the utility gain vs. utility loss yielded by the charging behavior of WCV.
- Second, the solution space of CEO problem is infinite since the sojourn spots are chosen in the continuous space which has infinite candidate locations, leading to extremely high computational complexity.
- Third, our proposed practical monitoring model increases the nonlinearity of the objective function in CEO problem (see Equation (13)) and introduces extra difficulty to analyze its monotonicity and submodularity.
- Fourth, scheduling the traveling tour of WCV among selected sojourn spots is similar to solving a Traveling Salesman Problem (TSP), which is NP-Hard. Thus CEO problem is the coupling of multiple challenging problems that cannot be solved straightforwardly.

To tackle these challenges, we design a charging utility model in which the utility gain and loss are simultaneously considered. We approximate the charging power through area discretization and investigate the routing problem of WCV. Through theoretical analysis of the objective function, an approximation algorithm is proposed which selects appropriate sojourn spots for WCV to maximize the charging utility. The main contributions of this paper are listed as follows:

- To the best knowledge of the authors, this is the first time the charging exclusivity issue is investigated. To tackle the exclusivity problem with COTS equipment in stochastic event monitoring, we trade off charging benefit and incidental loss and formalize the CEO problem to maximize the charging utility.
- By considering the charging exclusivity constraint, we propose a practical-application-oriented stochastic event monitoring model for WRSNs in which events are detected by surrounding sensors with probabilities less than 1. Through our strenuous efforts on theoretical analysis, it is proved that monotonicity and submodularity are still held for the objective utility function $U(X)$.
- To solve the proposed CEO problem, we reduce the candidate locations from infinite to finite with bounded error and transform the initial problem into maximization of a submodular function. We prove that with a slightly relaxed budget, the output of our proposed approximation algorithm is better than $(1-\epsilon)(1-1/e)/2$ of the optimal solution to the original problem with a smaller WCV charging radius $(1-\xi)D_c$.

II. Related Work

In this section, we mainly review the related work on mobile charging, which concentrated on different charging patterns. Existing research works mainly fall into two categories: online scheduling [17]–[20] and offline scheduling [9], [21], [22].

In online scheduling, rechargeable sensors send charging requests when their energy level falls below a certain threshold. Then the WCV schedules its traveling and charging behavior in a timely manner to serve the panic sensors. Lin *et al.* [23] explored the scheduling scheme for multiple WCVs based on joint temporal and spatial priorities of charging requests to maximize the survival rate of sensors. Fu *et al.* [18] tackled the unique design challenge for WRSN deployment through minimizing the charging delay by planning the optimal movement strategy of the mobile charger.

In offline scheduling [10], [11], one or more WCVs plan their traveling and charging behaviors through known sensors' information (such as energy status, locations, and energy consumption rate) in a priori. Wu *et al.* [21] focused on the collaborated tasks-driven mobile charging to improve the task utility. Liang *et al.* [24] investigated the charging rewards maximization problem utilizing a mobile charger with different amount of energy charged to sensors. Zhang *et al.* [25] minimized the energy cost due to the mobile chargers' movement and wireless charging loss so as to serve more charging requests.

Prior arts have made extraordinary contributions to WRSN performance improvement. However, the common problem of these prior works is that they *did not take charging exclusivity into consideration which exists in COTS applications.*

III. Model and Problem Statement

A. Network Model

As shown in Figure 1, there are m practical Point of Interests (denoted as $O = \{o_1, o_2, ..., o_m\}$) in a 2D plane network. Each PoI has a stochastic event arrival rate λ_i, which indicates the frequency of event that happens at its location. We consider n stationary rechargeable sensors (denoted as $S = \{s_1, s_2, ..., s_n\}$) deployed randomly in the network to monitor the occurrence of stochastic events of PoIs. Sensors are equipped with rechargeable batteries with capacity c and are implemented with S-MAC [26] and DD [27] protocols. A wireless charging vehicle (WCV) with a limited energy budget B, is employed as a mobile charger for providing energy replenishing service for sensors. Each time, a WCV starts from the base station and travels at a constant speed v along a number of selected sojourn spots (denoted as $X = \{x_1, x_2, ..., x_p\}$) to replenish sensors wirelessly and returns to base station before its energy approaches exhausted.

B. Event Model and Utility Computation

In this subsection, we introduce our stochastic event model and corresponding event monitoring utility computation.

TABLE I
SYMBOLS AND DEFINITIONS

Symbols	Definitions
o_i, O	a PoI, set of PoIs
s_j, S	a sensor, set of sensors
x_k, X	a sojourn spot, set of selected sojourn spots
$e(s_j, x)$	Charging power from WCV at x to sensor s_j
α	Traveling cost of WCV per unit length
β	Charging power of wireless charger on WCV
τ_k	Charging time at sojourn spot x_k
$C_k^{(c)}$	Charging cost of WCV at sojourn spot x_k
$C^{(t)}(X)$	Traveling cost of WCV with sojourn spot set X
$\mathcal{L}(X)$	Length of the path formed by spots in X
P_{ij}	Monitoring probability of sensor s_j to PoI o_i
S_i	Monitoring sensor set of o_i
$P_i(t)$	Monitoring probability of o_i
$P'_i(X, t)$	Monitoring probability of o_i after WCV charging at sojourn spot set X
T_i	Lifetime of o_i
U_i	Monitoring utility of o_i
$U'_i(X)$	Monitoring utility of o_i after WCV charging at sojourn spot set X
$U(X)$	Charging utility with respect to sojourn spot set X
c	Energy capacity of sensor
B	Energy capacity of WCV
σ	Number of edges of polygons
z_k, Z	Discrete subarea z_k, set of subareas

In our scenario, for a PoI, stochastic events occur with equal probability on it. In addition, we assume that event occurs *independently* with each other in both temporal and spatial dimensions [28], [29]. Under this assumption, the event generation process at a single PoI follows a Poisson process [30]. We assume that each sensor continuously perceives information from surrounding environment and generates utility when events occur within its coverage area during its lifetime.

The number of events that occur at a PoI within time interval $[s, s+t]$ obeys Poisson distribution

$$P(N(t) = n) = \frac{(\lambda t)^n e^{-\lambda t}}{n!}, \tag{1}$$

where λ is the arrival rate, which represents the number of events that occur per unit time.

Additionally, each event endures a certain period of time after its occurrence at a PoI. The duration time is considered as a random variable whose probability density function is denoted as $f(\cdot)$. For instance, we have $f(x) = \psi e^{-\psi x}$ when event duration follows exponential distribution.

Afterwards, we introduce the utility computation for our stochastic event model. In the network, sensor nodes are considered to monitor events at PoIs *independently* with certain probabilities during its lifetime. Specifically, the monitoring probability of sensor s_j to PoI o_i is P_{ij}. When a sensor exhausts its energy, it no longer conducts sensing tasks and thereby the monitoring probability is 0. Consequently, we denote $P_{ij}(t)$ as the monitoring probability:

$$P_{ij}(t) = \begin{cases} P_{ij}, & working, \\ 0, & exhausted. \end{cases} \tag{2}$$

Here, P_{ij} is a known value which is determined by hardware configurations and the distance from the sensor to PoI as well as environmental characteristics.

Constrained by the charging exclusivity issue, sensors cannot conduct sensing tasks while being charged. Thus, the monitoring probability after charging scheduling is

$$P'_{ij}(t) = \begin{cases} P_{ij}, & working, \\ 0, & being\ charged\ or\ exhausted. \end{cases} \tag{3}$$

For each PoI, we define a monitoring set of sensors as $S_i = \{s_j | d(s_j, o_i) \leq D_s\}$, which represents the sensors that are able to monitor PoI o_i. Here, $d(s_j, o_i)$ is the distance between s_j and o_i and D_s is the sensing range of sensors.

Since sensors monitor events independently with each other, the probability that events occurring at o_i are monitored by sensors in set S_i can be calculated by multiplication of monitoring probabilities of sensors in S_i. Thus, the probability $P_i(t)$ that events occurring at o_i are monitored is denoted as

$$P_i(t) = 1 - \prod_{s_j \in S_i} (1 - P_{ij}(t)). \tag{4}$$

After WCV has finished charging tasks at all sojourn spots in X, some nodes in S_i may have non-working periods since they cannot conduct monitoring tasks while being charged. Taking this issue into account, the probability of monitoring o_i by S_i is

$$P'_i(X, t) = 1 - \prod_{s_j \in S_i} (1 - P'_{ij}(t)). \tag{5}$$

We define the lifetime T_i of a PoI o_i as the longest lifetime of all sensors that can monitor it. In other words, when all sensors around the PoI are exhausted, the PoI will not be monitored, leading to event missing. Thus we have

$$T_i = max\{t_j | s_j \in S_i\}, \tag{6}$$

where t_j is the lifetime of sensor s_j.

We note that when WCV is fulfilling charging tasks, it will charge all sensors within its charging range to the full capacity. Thus charging performance will prolong the sensors' lifetime as well as the PoIs' lifetime.

Similar to [31], in our model, the monitoring utility of PoI o_i per unit time is a monotone concave function of $P_i(t)$, *i.e.*, $u(P_i(t))$. Suppose that an event starts at time t_s and ends at t_e. We denote $t_b = min\{t_e, T_i\}$ as the time point when utility is no longer generated. Thereby, its monitoring utility is calculated by $\int_{t_s}^{t_b} u(P_i(t))dt$ and the event duration time is $t_e - t_s$, with corresponding probability density $f(t_e - t_s)$. Since event duration follows probability function $f(x)$, the expectation of monitoring utility of an event is $\int_{t_s}^{\infty} \int_{t_s}^{t_b} u(P_i(t))dt f(t_e - t_s)dt_e$. At PoI o_i whose event arrival rate is λ_i, monitoring utility is generated for all events occur within its lifetime T_i. Considering all possible events that occur in $[0, T_i]$, the total monitoring utility of o_i through T_i is

$$U_i = \lambda_i \int_0^{T_i} \int_{t_s}^{\infty} \int_{t_s}^{t_b} u(P_i(t))dt f(t_e - t_s)dt_e dt_s. \tag{7}$$

Accordingly, the total monitoring utility of o_i (after WCV has finished charging tasks at all sojourn spots in X) is

$$U'_i(X) = \lambda_i \int_0^{T'_i} \int_{t_s}^{\infty} \int_{t_s}^{t_b} u(P'_i(X, t))dt f(t_e - t_s)dt_e dt_s. \tag{8}$$

Thereby we obtain the monitoring utility gain through charging process (*i.e.*, $U_i'(X) - U_i$), which represents the *charging utility*. Thus, we have tackled the first challenge described in Section I.

C. Charging Model

We consider that the wireless charging power from WCV to sensor decreases as their distance increases [10], [14]. When the power reduces to a certain value, it will not be obtained by sensors. Specifically, similar to [9], [32], the charging model is described as

$$e(s_j, x) = \begin{cases} \frac{\varphi}{(\delta + d(s_j, x))^2}, & d(s_j, x) \le D_c, \\ 0, & d(s_j, x) > D_c. \end{cases} \tag{9}$$

Here, φ and δ are constants configured by hardware and environment, respectively. D_c is the charging radius of WCV. When the distance between charger and sensor exceeds this value, the charging power can be negligible (*i.e.*, 0).

D. Energy Consumption of WCV

The energy cost of WCV mainly consists of two components: charging cost and traveling cost. Charging cost is the energy consumption when the WCV serves all the sensors nearby, which can be denoted as

$$C_k^{(c)} = \beta \cdot \tau_k. \tag{10}$$

Here β is the charger's power, $\tau_k = max_{s_j \in S_k^{(c)}} \frac{c - e_j}{e(s_j, x_k)}$ is the charging time spent at spot x_k, where $S_k^{(c)} = \{s_j | d(s_j, x_k) \le D_c\}$ and e_j is the residual energy of sensor s_j.

Traveling cost refers to the energy consumed by WCV when traveling around selected sojourn spots, which is represented by

$$C^{(t)}(X) = \alpha \cdot \mathcal{L}(X \cup \{BS\}). \tag{11}$$

Here $\mathcal{L}(X \cup \{BS\})$ is the length of the path through base station and spots in X, α is the traveling energy consumption per unit length.

E. Problem Formulation

Define the energy capacity of the WCV as B. In the charging and traveling process, the total cost should not exceed the capacity, hence we have

$$C^{(t)}(X) + \sum_{x_k \in X} C_k^{(c)} \le B. \tag{12}$$

Our problem here is *how to select the appropriate sojourn spots set X for WCV to charge surrounding sensors such that the total charging utility of the network is maximized.* Here, total charging utility $U(X)$ is defined as the sum of charging utility of each PoI. Thus we formulate the Charging Exclusivity Optimization (CEO) problem as

$$\begin{aligned} (\textbf{CEO}) \quad & \max \; U(X) = \sum_{o_i \in O} (U_i'(X) - U_i) \\ & s.t. \quad C^{(t)}(X) + \sum_{x_k \in X} C_k^{(c)} \le B. \end{aligned} \tag{13}$$

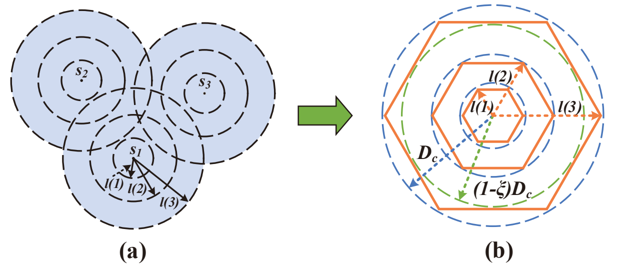

Fig. 2. Area discretization: (a) Draw concentric circles; (b) Replace circles by inscribed regular polygons.

F. Difficulty Analysis

To solve the CEO problem, we face several challenges here:

- When solving the CEO problem, we need to select several locations in the continuous space as sojourn spots. Obviously, the number of candidate locations is infinite (*i.e.*, the solution space of the problem is infinite, resulting in very high computational complexity). Therefore, the results cannot be obtained within polynomial time.
- The proposed practical monitoring model increases the nonlinearity of the objective function in CEO problem. Thereby, it is quite difficult to analyze its properties.
- In addition, since we analyze the traveling cost of WCV, we need to calculate the optimal path through selected sojourn spots, which again introduces another TSP problem [33], which is also NP-hard.

Therefore, the CEO problem is the coupling of multiple challenging problems that has high computational complexity.

IV. Our Scheme

A. Area Discretization and Problem Reformulation

To discretize the 2D continuous plane, a straightforward method here is to utilize a piecewise constant function to approximate the charging power (as shown in Figure 2(a)), thereby reducing the solution space of the problem.

Our aim is to segment the continuous region into pieces. First, to ensure the approximation rate, we need to determine the number of segments Q. We divide the WCV charging radius D_c into Q segments with endpoints: $l(0), l(1), ..., l(Q)$, which are ordered in an increasing order with $l(0)$ as the nearest endpoint and $l(Q)$ as the farthest.

Firstly, similar to [34], we take the location of sensors as the center of circles and draw concentric circles with radius $l(1), ..., l(Q)$ for each sensor (see Figure 2(a)). Thereby the approximated charging power of the charger located at any point between adjacent circles is regarded as uniform.

Afterwards, as shown in Figure 2(b), we replace the concentric circles (blue disks) by a series of inscribed regular polygons with σ edges (here, $\sigma = 6$) for simplicity to solve the routing problem (see Section IV-B). Thereby, the 2D plane is divided into several polygon areas. For s_j, we denote these areas as $H_1^j, H_2^j, ..., H_Q^j$, correspondingly. Similar to the above-mentioned, charging power at any point between adjacent polygons is regarded as uniform.

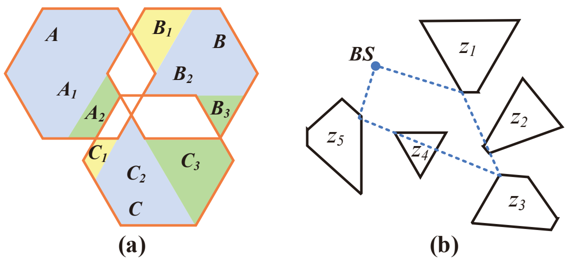

Fig. 3. Convex polygon partition: (a) Divide areas into convex polygons; (b) Touring among disjoint convex polygon areas.

We define the following approximation of charging power and bound its approximation error.

Definition 1: Letting $l(0) = 0$, $l(Q) = D_c$, and $l(q) = \delta\frac{\Gamma^q - 1}{\Gamma - 1}((1-\epsilon)^{-1/2} - 1)$, $(q = 1, ..., Q-1)$, where $\Gamma = \frac{\cos\frac{\pi}{\sigma}}{\sqrt{1-\epsilon}}$, the discrete charging power can be formally expressed by the following piecewise constant function:

$$e_r(s_j, x) = \begin{cases} e(l(1)), & x \in H_1^j \\ e(l(q)), & x \in H_q^j \backslash H_{q-1}^j \ (q = 1, ..., Q) \\ 0, & x \notin H_Q^j. \end{cases} \quad (14)$$

With $e_r(s_j, x)$, the approximated charging power can achieve $(1-\epsilon)$ approximation ratio to the actual charging power. Here, ϵ is a given error threshold. Relevant proof are given in Section V.

Naturally, the $(1-\epsilon)$ approximation ratio holds for the inner polygon areas $(H_1^j, H_2^j, ..., H_{Q-1}^j)$. For the outermost polygon area H_Q^j, when σ is large enough, although H_Q^j cannot cover the whole charging range (the outermost blue disk in Figure 2(b)), our scheme's performance is better than the case where D_c is slightly reduced to $(1-\xi)D_c$ (the green disk), where ξ is a small positive number.

Without loss of generality, we further partition the non-convex polygon areas into smaller convex polygon subareas. Taking Figure 3(a) as an example, non-convex areas A, B, and C are divided into convex subareas, *i.e.*, (A_1, A_2), (B_1, B_2, B_3), and (C_1, C_2, C_3), respectively. After partition, the 2D plane is finally divided into several convex polygon areas, which are denoted as $Z = \{z_1, z_2, ..., z_h\}$. We note that the charging power of each convex subarea is the same as the original area, *e.g.*, charging power in B_1, B_2, and B_3 is the same as B.

After area discretization, we convert the CEO problem into selecting subareas from a finite subarea set Z rather than directly selecting locations in the continuous 2D plane, which greatly reduces computational overhead. Thereby, our proposed CEO problem can be reformulated as

$$\begin{aligned} (\textbf{CEO-R}) \quad \max \quad & U(Z') = \sum_{o_i \in O} (U_i'(Z') - U_i) \\ s.t. \quad & C^{(t)}(Z') + \sum_{z_k \in Z'} C_k^{(c)} \leq B. \end{aligned} \quad (15)$$

Here, Z' is the set of selected subareas.

The CEO-R problem is a nonlinear combinatorial optimization problem, which falls into the scope of maximizing a submodular function with general routing constraints and can be approximately solved through our proposed algorithms (see Section IV-B and Section IV-C). Related definitions and proofs are given in Section V. Thereby, we have successfully solved the second and third challenges described in Section I.

B. Traveling Path Construction

To solve the last challenge, a compulsory work is to construct the shortest Hamiltonian cycle among selected sojourn spots, ensuring that the traveling cost is no more than an energy threshold. In fact, this problem is similar to the Traveling Salesman Problem (TSP). However, after area discretization, we should deal with the issue of scheduling WCV's traveling path among selected sojourn areas rather than spots. Thereby, the TSP problem is converted into a Touring Polygons Problem (TPP) [35], [36]. As shown in Figure 3(b), we try to find a path of minimum length that starts from a given spot (*i.e.*, base station), visits each of the disjoint convex polygons (*i.e.*, z_1 to z_5), and returns to the spot.

Without loss of generality, we assume that WCV will not stop at the boundaries of selected sojourn subareas. Thus, the areas can be regarded as pairwise disjoint convex areas. We use the geometric center of each subarea as a representative point to determine the traversal sequence. Afterwards, we can obtain the optimal path among them in this sequence within polynomial time referring to [36]. Afterwards, we randomly select a point within each sojourn area as the WCV's sojourn spot, which should locate in the intersection of the obtained path and the corresponding area.

The traveling cost is calculated corresponding to the obtained traveling path. We denote the total cost of WCV with selected sojourn area set Z' as

$$C(Z') = C^{(t)}(Z') + \sum_{z_k \in Z'} C_k^{(c)}. \quad (16)$$

C. Approximation Algorithm

Obviously, the two subproblems of our reformulated CEO-R problem (*i.e.*, WCV's sojourn areas selection problem and routing problem) are mutually coupled. In essence, different sojourn areas $z_1, z_2, ..., z_h$ will produce different traveling paths, while generating different traveling cost, which in turn affects the selection of sojourn areas. Thus the two subproblems need to be solved simultaneously.

In our solution, through area discretization, CEO-R problem falls into the scope of maximizing a submodular function with general routing constraints, which allows us to solve the problem by utilizing an approximation algorithm referring to the idea in [37]. In our proposed approximation algorithm, the two subproblems are considered simultaneously and a greedy strategy is adopted to iteratively select sojourn areas. In the k-th iteration, a sojourn area z_k is selected and added into the current set such that the cost-benefit ratio is maximized, *i.e.*,

$$z_k = \arg\max_{z \in Z \backslash Z'_{k-1}} \frac{U(Z'_{k-1} \cup \{z\}) - U(Z'_{k-1})}{C(Z'_{k-1} \cup \{z\}) - C(Z'_{k-1})}. \quad (17)$$

Algorithm 1 Approximation Algorithm for CEO-R Problem

```
Input: The monitoring probability $P_{ij}(t)$ of sensor $s_j$ to PoI $o_i$, the arrival rate $\lambda_i$ of PoI $o_i$, the parameters of charging model $\varphi$, $\delta$, energy consumption coefficient $\alpha$, $\beta$, sensors' battery capacity $c$, residual energy $e_j$ of sensor $s_j$ and energy budget $B$.
Output: The selected sojourn area set $Z'$, total charging utility $U(Z')$.
Discretize the network plane into subareas by drawing concentric circles with radius $l(1), ..., l(Q)$ for each sensor;
Let $Z'_0 \leftarrow \varnothing$, $C(Z') \leftarrow 0$, and $\mathcal{Z} \leftarrow \text{argmax}\{U(z_k)|z_k \in Z, C(Z'_k) \leq B\}$;
while $Z \neq null$ do
    for $\forall z \in Z$ do
        Compute the charging utility $U(Z'_{k-1} \cup \{z\})$ and $U(Z'_{k-1})$ with corresponding monitoring utility;
        Compute the total cost $C(Z'_{k-1} \cup \{z\})$ and $C(Z'_{k-1})$ with the obtained path among corresponding sojourn areas;
    end for
    $z_k \leftarrow \arg\max_{z \in Z \backslash Z'_{k-1}} \frac{U(Z'_{k-1} \cup \{z\}) - U(Z'_{k-1})}{C(Z'_{k-1} \cup \{z\}) - C(Z'_{k-1})}$;
    if $z_k \leq 0$ then
        break;
    end if
    if $C(Z'_k \cup \{z_k\}) \leq B$ then
        $Z'_k \leftarrow Z'_k \cup \{z_k\}$;
        $k \leftarrow k + 1$;
    end if
    $Z \leftarrow Z \backslash \{z_k\}$;
end while
$Z' \leftarrow Z'_k$;
if $U(\mathcal{Z}) \geq U(Z')$ then
    $Z' \leftarrow \mathcal{Z}$;
end if
Output $Z', U(Z')$;
```

We define $Z'_0 = \varnothing$ as the initial sojourn area set and $Z'_k = \{z_1, z_2, ..., z_k\}$ as the selected set in iteration k. We note that the cost $C(Z'_k)$ is calculated in each iteration. Every time a new sojourn area is selected and added into the current set Z'_{k-1}, the Hamiltonian cycle among current areas is generated and traveling cost is obtained correspondingly.

The iteration process will continue until the energy constraint is exceeded. We obtain the sojourn area set Z'_k, satisfying: $C(Z'_k) \leq B$ and $C(Z'_{k+1}) \geq B$. $\mathcal{Z}$ only contains a single sojourn area. We compare $U(Z'_k)$ with $U(\mathcal{Z})$ and choose the maximum one as the result set. The details of the algorithm are described in Algorithm 1. Thereby, we have tackled all the challenges of CEO problem and the performance of our scheme is verified theoretically in the followings.

V. Theoretical Analysis

In this section, we describe how charging behaviors can increase the monitoring utility of PoIs by affecting the lifetime of sensors, and thereby prove the properties of the charging utility function $U(X)$.

When WCV is performing charging tasks, it will charge all sensors within its charging range to full capacity. Constraint by the charging exclusivity issue, monitoring events and harvesting energy cannot be conducted simultaneously by a sensor. Thereby, as shown in Figure 4, charging behavior will cause temporary monitoring loss during the charging process, meanwhile prolonging the PoI's lifetime, and the overall monitoring utility is raised. To quantitatively describe the influence produced by charging exclusivity, we define the charging utility function $U(X)$, which is the objective function of the proposed CEO problem. Then we deeply explore the characteristic of $U(X)$ which enables us to transform the original problem into a submodular function maximization problem with routing constraints.

***Definition 2*: (Nonnegativity, Monotonicity, and Submodularity)** Given a finite ground set $\mathcal{V}$, a real-valued set function is defined as $f : 2^{\mathcal{V}} \rightarrow R$, f is called *nonnegative*, *monotone (nondecreasing)*, and *submodular* if and only if it satisfies following conditions, respectively.

- $f(\varnothing) = 0$ and $f(A) \geq 0$ for all $A \subseteq \mathcal{V}$ *(nonnegative)*;
- $f(A) \leq f(B)$ for all $A \subseteq B \subseteq \mathcal{V}$ or equivalently: $f(A \cup \{e\}) - f(A) > 0$ for all $A \subseteq \mathcal{V}$ and $e \in \mathcal{V} \backslash A$ *(monotone)*;
- $f(A) + f(B) \geq f(A \cup B) + f(A \cap B)$, for any $A, B \subseteq \mathcal{V}$ or equivalently: $f(A \cup \{e\}) - f(A) \geq f(B \cup \{e\}) - f(B)$, $A \subseteq B \subseteq \mathcal{V}$, $e \in \mathcal{V} \backslash B$ *(submodular)*;

Through profound analysis of the characteristics of $U(X)$, we have the following theorem:

Theorem 1: The charging utility function $U(X)$ in CEO problem is nonnegative, monotone, and submodular.

Proof: Apparently, $U(\varnothing) = 0$, as no charging means no charging utility. Due to the monotonicity of $U(X)$, we have $U(X) \geq 0$. Thus the nonnegativity holds for $U(X)$.

Since the total charging utility of the network is the sum of utility of each PoI and U_i is a constant (see Equation (7)), we prove the monotonicity and submodularity of $U'_i(X)$ to represent the total utility $U(X)$.

Without loss of generality, we reformulate the objective function $U'_i(X)$ into the form of $h(\mathcal{U}(X))$, in which $h(\cdot)$ is a monotone concave function. Then we prove *Theorem 1* by indicating the nonnegativity, monotonicity and submodularity of substitute function $\mathcal{U}(X)$.

For a stochastic event, we consider its duration as a random variable whose expectation is $E = \int_{t_a}^{\infty} (t_b - t_a) f(t_b - t_a) dt_b$, and $U'_i(X)$ is reformulated as

$$U'_i(X) \propto \int_0^{T'_i} \int_t^{t+E} u(P'_i(X, x)) dx dt \tag{18}$$

$$\propto E \int_0^{T'_i} u(P'_i(X, x)) dx \tag{19}$$

$$\propto h(\int_0^{T'_i} P'_i(X, x) dx). \tag{20}$$

Since arrival rate λ_i is a constant for PoI o_i and function $u(\cdot)$ is a monotone concave function, we have Equation (18). It is noted that $P'_i(x)$ is a piecewise constant function, thus Equation (19) can be proved. We omit this proof due to the space limitation. Based on the above derivation, we have Equation (20) in which $\mathcal{U}(X) = \int_0^{T'_i} P'_i(X, x) dx$ and $U'_i(X) = h(\mathcal{U}(X))$.

Actually, for a PoI whose lifetime is T'_i, events occurring within time period $[-E, T'_i)$ can be monitored. For simplicity, we only consider the events that occur in $[0, T'_i)$ since E is significantly shorter than T'_i.

Here we prove the monotonicity and submodularity of function $\mathcal{U}(X)$. Without loss of generality, we assume that

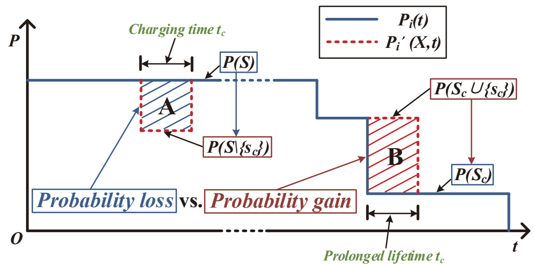

Fig. 4. Probability gain and probability loss in different time periods.

all charged nodes have the same length of lifetime as they own identical energy capacity.

Monotonicity: Comparing with the lifetime of a sensor, the time duration of charging scheduling is rather short. Thereby we consider that no sensor will exhaust its energy during the charging scheduling period.

For easy proof, we assume that when WCV charges at sojourn spot x_k, the charging power is 0 and one sensor s_c is charged. Under this assumption, charging behavior is equivalent to turning the sensor off for a while (charging time t_c) and reopening it. In other words, the time at which the sensor exhausts its energy is delayed by t_c and the total working time does not change, as shown in Figure 4. Time slot t_c is moved from the beginning of charging to the end of its lifetime, thus generating probability loss (area A) and probability gain (area B) at corresponding time periods.

We denote $P(S)$ as the total monitoring probability when sensors in set S are monitoring a PoI simultaneously. Intuitively, $P(S)$ is a submodular function. The probability loss in charging period is $P(S)-P(S\backslash\{s_c\})$ (the height of area A). When s_c exhausts its energy, sensors that are still alive form a subset of $S\backslash\{s_c\}$, which is denoted as S_c. The probability gain in prolonged lifetime t_c is $P(S_c\cup\{s_c\})-P(S_c)$ (the height of area B). Since S_c is a subset of $S\backslash\{s_c\}$, according to Equation (4), we have $P(S_c\cup\{s_c\})-P(S_c) \geq P(S)-P(S\backslash\{s_c\})$ due to submodularity of function $P(S)$, which indicates that the probability gain is greater than probability loss. This inequality still holds when multiple sensors are charged. We omit the proof due to space limitation. Thereby, we have

$$\mathcal{U}(X \cup \{x_k\}) - \mathcal{U}(X) \geq 0.$$

Since the monotonicity holds for $\mathcal{U}(X)$ under the consumption of zero charging power, it is obvious that this property still holds when charging power is greater than 0.

Therefore, we prove that $\mathcal{U}(X)$ is monotone.

Submodularity: We consider two conditions A and B, under which the sojourn area sets are A and B respectively ($A \subseteq B \subseteq \mathcal{V}$). Moreover, a newly added area $e \in \mathcal{V}\backslash B$ is considered. Let S_A, S_B, and S_e denote the sensor set that WCV can charge at areas A, B, and e respectively. Apparently, there is $S_A \subseteq S_B$.

(Case 1) Firstly, we consider the case where $S_e \subseteq S_A$, which means that all sensors in S_e have been charged under condition A and B. We note that charging the same sensor once and multiple times are equivalent. Thus we have

$$\mathcal{U}(A \cup \{e\}) - \mathcal{U}(A) = \mathcal{U}(B \cup \{e\}) - \mathcal{U}(B) = 0.$$

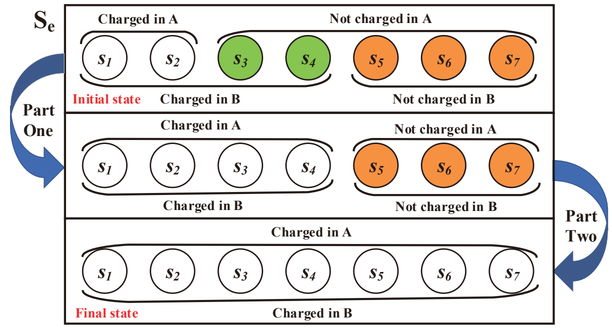

Fig. 5. Detailed charging process in **(Case 3)**.

(Case 2) Secondly, we consider the case where $S_e \subseteq S_B$ and $S_e \nsubseteq S_A$. In this case, all sensors in S_e have been charged under condition B. Thus, we have $\mathcal{U}(B \cup \{e\}) - \mathcal{U}(B) = 0$. Some sensors in S_e have not been charged under condition A. Due to the monotonicity, $\mathcal{U}(A\cup\{e\})-\mathcal{U}(A) \geq 0$ is satisfied. Thereby we have

$$\mathcal{U}(A \cup \{e\}) - \mathcal{U}(A) \geq \mathcal{U}(B \cup \{e\}) - \mathcal{U}(B).$$

(Case 3) Thirdly, we consider the case where $S_e \nsubseteq S_B$ and give an example in Figure 5. We assume that there are seven sensors in S_e, and two of them (s_1 and s_2) are charged in A while four of them (s_1, s_2, s_3, and s_4) are charged in B. Since $S_A \subseteq S_B$, we have $\|S_e - S_A\| \geq \|S_e - S_B\|$, which indicates that when WCV charges at sojourn area e, the number of newly charged sensors under condition A (s_3 to s_7) is more than that under condition B (s_5 to s_7). We separate the charging process into two parts. In part one, sensors in set $(S_e-S_A)\backslash(S_e-S_B)$ (s_3 and s_4) are charged. In part two, the residual sensors in set $S_e - S_A$ (s_5 to s_7) are charged.

In the first part of the charging process, sensors in set $(S_e - S_A)\backslash(S_e - S_B)$ (s_3 and s_4) are charged. Charging utility is generated for A due to the monotonicity of the utility function. Nevertheless, there is no charging utility for B since no sensor is newly charged.

Therefore, *the charging utility in part one for A is greater than that for B.*

We analyze the second part of the charging process, in which the same sensors (s_5 to s_7) are charged under both condition A and B. For a given PoI o_i, which is monitored by sensors in set $S_i = \{s_1, s_2, ..., s_n\}$, some sensors in S_i have been charged under condition A and more sensors have been charged under condition B. Meanwhile, a subset of S_i is newly charged for both A and B, which is denoted as S_{charge} (in our example, $S_{charge} = \{s_5, s_6, s_7\}$). The probability loss in charging period is $P(S_i) - P(S_i\backslash S_{charge})$, which is equivalent under condition A and B. Their probability gains in prolonged lifetime are $P(S_c^A \cup S_{charge}) - P(S_c^A)$ and $P(S_c^B \cup S_{charge}) - P(S_c^B)$, respectively. Since $S_A \subseteq S_B$, which means that more sensors' lifetime are prolonged under condition B, $S_c^A \subseteq S_c^B$ is proved. Thus, we have

$$P(S_c^A \cup S_{charge}) - P(S_c^A) \geq P(S_c^B \cup S_{charge}) - P(S_c^B).$$

Therefore, *the charging utility in part two for A is greater than that for B.*

Combining with the two parts of the charging process, in Case 3, we have

$$\mathcal{U}(A \cup \{e\}) - \mathcal{U}(A) \geq \mathcal{U}(B \cup \{e\}) - \mathcal{U}(B).$$

In summary, we prove that $\mathcal{U}(X)$ is submodular. Consequently, *Theorem 1* is proved. ■

Theorem 2: With $e_r(s_j, x)$, the approximation error of charging power in area discretization is subject to

$$1 - \epsilon \leq \frac{e_r(s_j, x)}{e(s_j, x)} \leq 1, (x \in H_Q^j). \tag{21}$$

Proof: To achieve the $(1-\epsilon)$ approximation ratio, we should ensure that within a subarea, the actual minimum charging power should not be lower than $1-\epsilon$ of the actual maximum charging power. Thus the charging power of adjacent subareas has the following relationship:

$$\frac{\varphi}{(\delta + l(q) \cdot \cos \frac{\pi}{\sigma})^2} \cdot (1 - \epsilon) = \frac{\varphi}{(\delta + l(q+1))^2}. \tag{22}$$

The maximum and the minimum charging power within the charging range are $\frac{\varphi}{(\delta+0)}$ and $\frac{\varphi}{(\delta+D_c)}$ accordingly. Combining these two expressions with Equation (9) and Equation (22), we can get the following equation:

$$l(q) = \delta \frac{\Gamma^q - 1}{\Gamma - 1}((1-\epsilon)^{-1/2} - 1), \tag{23}$$

where $\Gamma = \frac{cos\frac{\pi}{\sigma}}{\sqrt{1-\epsilon}}$. Thereby, we prove the $(1-\epsilon)$ approximation ratio of charging power in area discretization. ■

Theorem 3: With a slightly relaxed budget, the output of our proposed approximation algorithm is better than $(1-1/e)/2$ of the optimal solution to CEO problem with a smaller charging radius $(1-\xi)D_c$, and its time complexity is bounded to $O(n^6\epsilon^{-6}\nu)$.

Proof: According to Section IV-A, we have transformed the CEO problem into the maximization of a submodular function with routing constraints through area discretization. Therefore, according to [37], Algorithm 1 has a $(1-1/e)/2$ approximation ratio compared to the optimal solution.

Considering the approximation error induced by area discretization (see Section IV-A), the charging cost of WCV is higher than the actual charging cost but does not exceed $\frac{1}{1-\epsilon}$ of it. Together with the traveling cost error in path construction, therefore, we can obtain $(1-1/e)/2$ of the optimal solution with a slightly relaxed budget [37]. Finally, the output of our algorithm is better than $(1-1/e)/2$ of the optimal solution to CEO problem with a smaller charging radius $(1-\xi)D_c$.

It is noted that the number of polygon areas partitioned by all concentric polygons is $N = O(n^2\epsilon^{-2})$. Due to the space limitation, we omit the proof here. Although we further divide the non-convex polygon areas into convex subareas, we note that for each non-convex area, at most one of its subareas can be selected in Algorithm 1 since different subareas have different positions but own the same charging power. As a result, the maximum size of the selected sojourn area set is $N = O(n^2\epsilon^{-2})$. Hereby, Algorithm 1 has at most N iterations. In each iteration, the TPP problem is solved referring to [36], whose time complexity is $O(N\nu)$, where ν is the total number of vertices of the given polygon areas. Thus the overall time complexity is $O(n^6\epsilon^{-6}\nu)$. ■

VI. Simulation Analysis

We carry out extensive simulations to evaluate the performance of our proposed algorithm from various aspects. Several baseline algorithms are introduced for comparison.

A. Simulation Setup

As it is quite difficult or sometimes unreliable to generate stochastic events with simulators, we utilize real statistical data of epilepsy patients as the stochastic events data in our simulations [38]. Specifically, frequency and duration time of the pathogenic behavior of epilepsy patients are utilized as event frequency and event duration time in our simulation.

In our simulation, we assume that there are 40 POIs randomly distributed in a $100m*100m$ area with one epilepsy patient represents each. We deploy 100 rechargeable sensors around the PoIs to detect the stochastic event occurring at them. A WCV travels within the area to charge sensors at selected sojourn areas. Meanwhile, we try to guarantee that all the stochastic events of the PoIs are detected by surrounding sensors, and try to avoid the monitoring failure due to charging exclusivity. The energy capacities of sensors and WCV are $c = 50$ and $B = 10000$, respectively. Relative parameters are set as: $\varphi = 15$, $\delta = 10$, $\alpha = 4$, $\beta = 0.5$, $\sigma = 10$, $D_c = 10m$, $v = 1.5m/s$, and $f(x) = e^{-x}$.

B. Baseline Setup

We compare our algorithm (CEO for short) with four baseline algorithms: ME, CCO, CHASE, and CHASE-C. ME (maximum energy algorithm) selects the sojourn areas at which WCV can achieve the largest amount of energy transmitted to surrounding sensors, regardless of incidental utility loss due to charging exclusivity. CCO (charging compatibility optimization) follows the same scheduling strategy as CEO and the only difference between them is CCO ignores the charging exclusivity issue (*i.e.*, charging and sensing can be conducted simultaneously) while CEO takes it into account. CHASE [39] is a state-of-the-art algorithm and CHASE-C is its ideal version. In CHASE algorithm, charging and sensing cannot be conducted simultaneously (leading to utility loss), while in CHASE-C, we assume that charging and sensing can take place simultaneously.

C. Simulation Results and Analysis

Generally, through extensive simulations, the numerical results (See Figure 6 to Figure 11) shows that if charging and sensing can be conducted simultaneously, CHASE-C and CCO both achieve higher charging utility than other three algorithms. However, when we take charging exclusivity into account, the results of CHASE and CEO are lower than CHASE-C and CCO, respectively. We note that although charging exclusivity leads to performance decline, the performance of CEO is obviously better than CHASE and ME by 21.3% on average in terms of charging utility.

Firstly, we analyze the impact of error threshold ϵ. As shown in Figure 6, when ϵ increases from 0.1 to 0.5, the charging utility of CHASE-C, CCO, CEO, CHASE, and

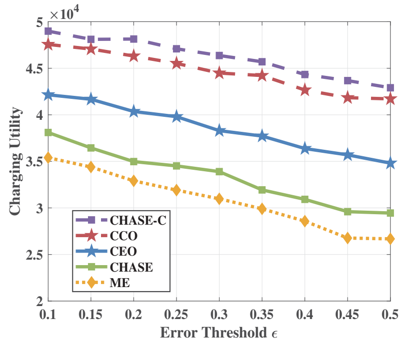

Fig. 6. Utility vs. ϵ.

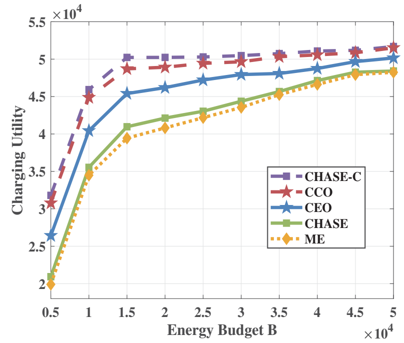

Fig. 7. Utility vs. B.

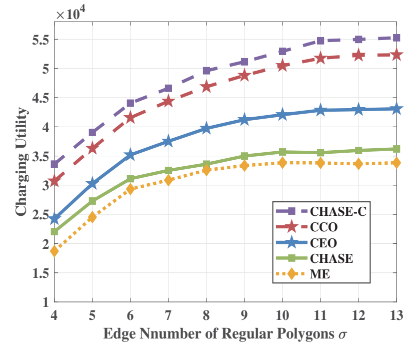

Fig. 8. Utility vs. σ.

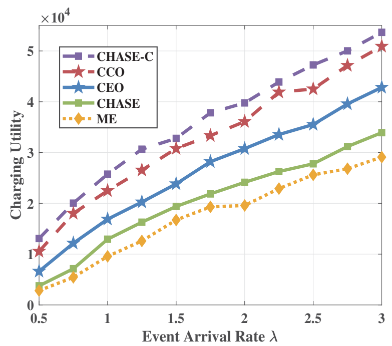

Fig. 9. Utility vs. λ.

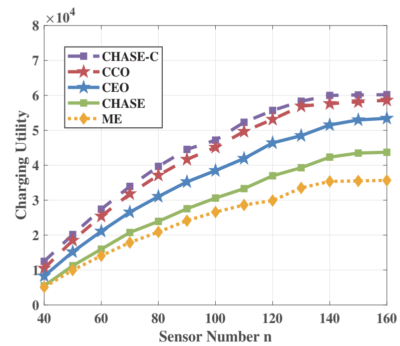

Fig. 10. Utility vs. n.

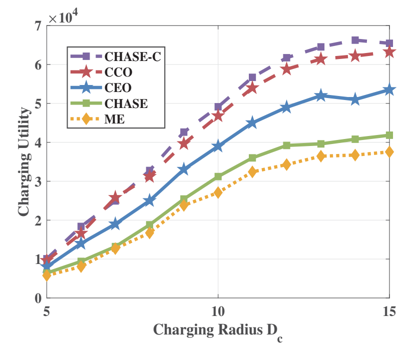

Fig. 11. Utility vs. D_c.

ME decreases gradually. It is noted that we discretize the area through charging power segmentation. In fact, practical charging power is approximated to a lower constant value. As ϵ rises, the discretization is getting more coarse-grained. Thereby charging power is more likely to be approximated to a much lower value, leading to the utility loss. With respect to the charging utility, CEO algorithm outperforms CHASE and ME by 20.6% on average.

Secondly, we analyze the impact of WCV's energy budget B. As shown in Figure 7, when B increases from $5,000$ to $50,000$, the charging utility of the five algorithms increases rapidly at the beginning and gradually stabilizes. Apparently, when the energy budget of WCV is promoted, it can select more sojourn areas and charge more sensors, leading to an increasing trend of charging utility. However, when the budget reaches a certain value, most sensors will be charged. As a result, enlarging the budget will not produce significant utility gain. On average, CEO algorithm outperforms CHASE and ME by 11.4% in charging utility.

Thirdly, we analyze the impact of the edge number of regular polygons σ. As shown in Figure 8, when σ increases from 4 to 13, the charging utility of the five algorithms rises dramatically at first and later grows stabilized. In area discretization, we draw concentric σ-edge regular polygons to segment the continuous charging power. When σ is larger, the polygon is more similar to a disk and thereby the approximated charging model is closer to the practical model. When the number of edges is more than 10, the increasing trend gradually weakens. CEO algorithm achieves 20.1% higher charging utility than CHASE and ME on average.

Fourthly, we analyze the impact of event arrival rate λ. As shown in Figure 9, when λ increases from 0.5 to 3, the charging utility of the five algorithms increases rapidly, since more frequent event occurrence provides more monitoring utility. Although the utility loss caused by charging exclusivity rises since there will be more event missing during charging, in the prolonged lifetime, sensors will produce more utility gain than aforementioned utility loss. Thereby the total charging utility is raised. Under this condition, CEO algorithm outperforms CHASE and ME by at least 22.9% in charging utility.

Afterwards, we analyze the impact of sensor number n. As shown in Figure 10, when n increases from 40 to 160, the charging utility of five algorithms shows an obvious growth trend. The reason is that with higher sensor density, WCV can charge more sensors at a time, thereby generating more charging utility. When sensor density increases to a certain extent, the monitoring probabilities of PoIs are close to 1. Then the growth trend slows down since charging more sensors will not significantly increase the monitoring probability and monitoring utility. From the aspect of sensor number, CEO algorithm outperforms CHASE and ME by at least 21.7%.

Finally, we analyze the impact of charging radius D_c. As shown in Figure 11, when D_c increases from 5 to 15, the charging utility of the five algorithms shows almost linear growth at the beginning, since WCV can charge more sensors within its charging radius, which increases the charging utility. However, it is noted that the charging power decreases with distance rapidly. Thereby, if the charging radius is too large, charging a faraway sensor to full capacity will spend a long time and waste large amounts of energy. As a result, the growth trend slows down when D_c increases to a certain value. We conclude that CEO algorithm outperforms CHASE and ME

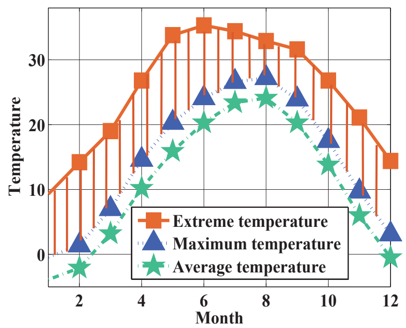

Fig. 12. Local temperature statistics.

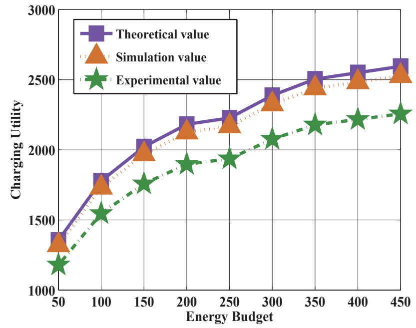

Fig. 13. Experiments vs. simulations vs. theoretical results.

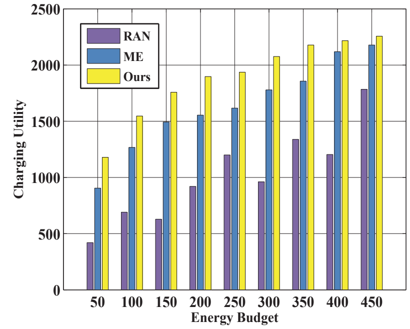

Fig. 14. Utility vs. Budget.

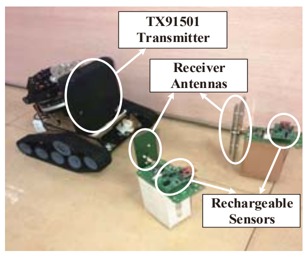

Fig. 15. Practical charging process.

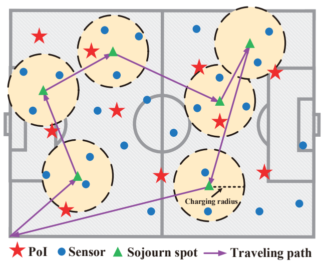

Fig. 16. Soccer field scenario.

by at least 24.9% in terms of charging utility.

VII. Test-bed Experiments

To demonstrate the feasibility of our scheme in realistic scenarios, we conduct test-bed experiments to evaluate its performance.

Our WRSN test-bed consists of several rechargeable sensors and one WCV, which are built with COTS devices. In detail, we utilize Powercast P2110-EVB as the power harvest module of sensor which can convert RF signal into DC power. The WCV is equipped with a TX91501 RF transmitter which can send out RF signals on 915MHz (see Figure 15).

In our experiment, we imitate the fire monitoring network. Specifically, we set 10 key monitoring spots in different locations within a soccer field (see Figure 16) as PoIs and deploy 25 rechargeable sensors around them. Sensors conduct sensing tasks by collecting temperature data of PoIs within its sensing range and send back packets to the base station. For comparison, we take the local temperature statistics (average temperature, maximum temperature, and extreme temperature) as a guideline (see Figure 12), and select the maximum temperature (the blue curve) as the judgment criteria of a critical event. When the temperature of a PoI falls in the shaded area in Figure 12, it is considered as an imitated fire.

The network deployment is shown in Figure 16. Our experiments were conducted in different weather conditions and lasted 45 days, during which charging utility was calculated and recorded under different WCV budget.

We compare the differences among theoretical, simulation, and experimental results on energy budget in Figure 13. In the theoretical analysis, the WCV traveling time is ignored, leading to the $3-15\%$ gap between theoretical results and simulation/experimental results. Our simulation and experimental results fit well with theoretical analysis, which demonstrates the feasibility of our scheme in realistic scenarios.

Then we analyze the charging utility obtained by three algorithms: Ours, RAN, and ME under different settings of energy budget. The RAN algorithm randomly selects sojourn areas for WCV to charge surrounding sensors until the energy budget of WCV is exceeded. As shown in Figure 14, when energy budget rises from 50 to 450, our proposed algorithm apparently outperforms ME and RAN.

VIII. Conclusions

In this paper, we propose the first scheme that quantitatively leverages the utility gain vs. incidental utility loss yielded by charging behavior of WCV and trades off charging and sensing to deal with the effect of charging exclusivity in stochastic events monitoring. Through critical discretization techniques and theoretical analysis, we transform the formulated CEO problem into maximization of a submodular function with routing constraints. With a slightly relaxed budget, our proposed approximation algorithm can achieve the solution better than $(1-1/e)/2$ of the optimal solution to CEO problem with a smaller charging radius $(1-\xi)D_c$. Extensive simulations are conducted based on practical data and numerical results show that our proposed algorithm outperforms baseline algorithms by 19.7% on average. Our test-bed experiments indicate the feasibility of our scheme in realistic scenarios.

Acknowledgments

This research is sponsored in part by the National Natural Science Foundation of China (61872052, 61872053, 61872178), National Key Research and Development Program (2017YFC0704200), the Xinghai Scholar Program in Dalian University of Technology, Fundamental Research Funds for the Central Universities (DUT19JC39, DUT19GJ204), Natural Science Foundation of Liaoning Province under Grant No.2019-MS-055, Youth Science and Technology Star of Dalian under Grant 2018RQ45, Opening Project of Shanghai Trusted Industrial Control Platform under Grant No.TICPSH202003017-ZC, "Dalian Science and Technology Innovation Fund" with No. 2019J11CY004the Fund of Acoustics Science and Technology Laboratory, and Science and Technology on Underwater Test and Control Laboratory with No. 6142407190510, Natural Science Foundation of Jiangsu Province under Grant No. BK20181251.

REFERENCES

[1] L. Xie, Y. Shi, Y. T. Hou, and W. Lou, "Wireless power transfer and applications to sensor networks," *IEEE Wireless Communications*, vol. 20, no. 4, 2013.

[2] P. Zhou, C. Wang, and Y. Yang, "Self-sustainable sensor networks with multi-source energy harvesting and wireless charging," in *IEEE INFOCOM*, 2019, pp. 1828–1836.

[3] L. Xie, Y. Shi, Y. T. Hou, W. Lou, H. D. Sherali, and S. F. Midkiff, "Bundling mobile base station and wireless energy transfer: Modeling and optimization," in *IEEE INFOCOM*, 2013, pp. 1636–1644.

[4] H. Dai, X. Wu, G. Chen, L. Xu, and S. Lin, "Minimizing the number of mobile chargers for large-scale wireless rechargeable sensor networks," *Computer Communications*, vol. 46, pp. 54–65, 2014.

[5] H. Dai, X. Wu, L. Xu, G. Chen, and S. Lin, "Using minimum mobile chargers to keep large-scale wireless rechargeable sensor networks running forever," in *IEEE ICCCN*, 2013, pp. 1–7.

[6] C. Lin, Z. Shang, W. Du, J. Ren, L. Wang, and G. Wu, "CoDoC: A novel attack for wireless rechargeable sensor networks through denial of charge," in *IEEE INFOCOM*, 2019, pp. 856–864.

[7] S. He, J. Chen, F. Jiang, D. K. Y. Yau, G. Xing, and Y. Sun, "Energy provisioning in wireless rechargeable sensor networks," *IEEE Transactions on Mobile Computing*, vol. 12, no. 10, pp. 1931–1942, 2013.

[8] H. Dai, G. Chen, C. Wang, S. Wang, X. Wu, and F. Wu, "Quality of energy provisioning for wireless power transfer," *IEEE Transactions on Parallel Distributed Systems*, vol. 26, no. 2, pp. 527–537, 2015.

[9] T. Wu, P. Yang, H. Dai, W. Xu, and M. Xu, "Charging oriented sensor placement and flexible scheduling in rechargeable wsns," in *IEEE INFOCOM*, 2019, pp. 73–81.

[10] C. Lin, Y. Zhou, F. Ma, J. Deng, L. Wang, and G. Wu, "Minimizing charging delay for directional charging in wireless rechargeable sensor networks," in *IEEE INFOCOM*, 2019, pp. 1819–1827.

[11] C. Lin, Y. Zhou, H. Dai, J. Deng, and G. Wu, "MPF: Prolonging network lifetime of wireless rechargeable sensor networks by mixing partial charge and full charge," in *IEEE SECON*, 2018, pp. 379–387.

[12] "Powercast," http://www.powercastco.com.

[13] J. R. Smith, A. P. Sample, P. S. Powledge, S. Roy, and A. V. Mamishev, "A wirelessly-powered platform for sensing and computation," in *ACM UbiComp*, 2006, pp. 495–506.

[14] H. Dai, Y. Zhao, G. Chen, W. Dou, C. Tian, X. Wu, and T. He, "Robustly safe charging for wireless power transfer," in *IEEE INFOCOM*, 2018, pp. 378–386.

[15] N. Yu, H. Dai, A. X. Liu, and B. Tian, "Placement of connected wireless chargers," in *IEEE INFOCOM*, 2018, pp. 387–395.

[16] H. Yigitler, O. Kaltiokallio, R. Hostettler, A. S. Abrar, R. Jäntti, N. Patwari, and S. Särkkä, "RSS models for respiration rate monitoring," *IEEE Trans. Mob. Comput.*, vol. 19, no. 3, pp. 680–696, 2020.

[17] P. Guo, X. Liu, S. Tang, and J. Cao, "Concurrently wireless charging sensor networks with efficient scheduling," *IEEE Transactions on Mobile Computing*, vol. 16, no. 9, pp. 2450–2463, 2017.

[18] L. Fu, P. Cheng, Y. Gu, J. Chen, and T. He, "Optimal charging in wireless rechargeable sensor networks," *IEEE Transactions on Vehicular Technology*, vol. 65, no. 1, pp. 278–291, 2016.

[19] C. Lin, S. Wei, J. Deng, M. S. Obaidat, H. Song, L. Wang, and G. Wu, "GTCCS: A game theoretical collaborative charging scheduling for on-demand charging architecture," *IEEE Transactions on Vehicular Technology*, vol. 67, no. 12, pp. 12 124–12 136, 2018.

[20] C. Lin, Y. Sun, K. Wang, Z. Chen, B. Xu, and G. Wu, "Double warning thresholds for preemptive charging scheduling in wireless rechargeable sensor networks," *Computer Networks*, vol. 148, pp. 72–87, 2019.

[21] T. Wu, P. Yang, H. Dai, W. Xu, and M. Xu, "Collaborated tasks-driven mobile charging and scheduling: A near optimal result," in *IEEE INFOCOM*, 2019, pp. 1810–1818.

[22] C. Lin, F. Gao, H. Dai, J. Ren, L. Wang, and G. Wu, "Maximizing charging utility with obstacles through fresnel diffraction model," in *IEEE INFOCOM*, 2020, pp. 2046–2055.

[23] C. Lin, Z. Wang, J. Deng, L. Wang, J. Ren, and G. Wu, "mTS: Temporal-and spatial-collaborative charging for wireless rechargeable sensor networks with multiple vehicles," in *IEEE INFOCOM*, 2018, pp. 99–107.

[24] W. Liang, Z. Xu, W. Xu, J. Shi, G. Mao, and S. K. Das, "Approximation algorithms for charging reward maximization in rechargeable sensor networks via a mobile charger," *IEEE/ACM Transactions on Networking*, vol. 25, no. 5, pp. 3161–3174, 2017.

[25] S. Zhang, Z. Qian, J. Wu, F. Kong, and S. Lu, "Optimizing itinerary selection and charging association for mobile chargers," *IEEE Transactions on Mobile Computing*, vol. 16, no. 10, pp. 2833–2846, 2017.

[26] W. Ye, J. S. Heidemann, and D. Estrin, "An energy-efficient MAC protocol for wireless sensor networks," in *IEEE INFOCOM*, 2002, pp. 1567–1576.

[27] C. Intanagonwiwat, R. Govindan, and D. Estrin, "Directed diffusion: A scalable and robust communication paradigm for sensor networks," in *ACM MOBICOM*, 2000, pp. 56–67.

[28] D. K. Y. Yau, N. K. Yip, C. Y. T. Ma, N. S. V. Rao, and M. Shankar, "Quality of monitoring of stochastic events by periodic and proportional-share scheduling of sensor coverage," *ACM Transactions on Sensor Networks*, vol. 7, no. 2, pp. 1–49, 2010.

[29] S. He, J. Chen, D. K. Y. Yau, H. Shao, and Y. Sun, "Energy-efficient capture of stochastic events by global- and local-periodic network coverage," in *ACM MobiHoc*, 2009, pp. 155–164.

[30] V. Rai and R. N. Mahapatra, "Lifetime modeling of a sensor network," in *DATE*, 2005, pp. 202–203.

[31] H. Dai, Q. Ma, X. Wu, G. Chen, D. K. Y. Yau, S. Tang, X.-Y. Li, and C. Tian, "CHASE: Charging and scheduling scheme for stochastic event capture in wireless rechargeable sensor networks," *IEEE Transactions on Mobile Computing*, 2019.

[32] H. Dai, Y. Liu, G. Chen, X. Wu, T. He, A. X. Liu, and Y. Zhao, "SCAPE: safe charging with adjustable power," *IEEE/ACM Transactions on Networking*, vol. 26, no. 1, pp. 520–533, 2018.

[33] D. Feillet, P. Dejax, and M. Gendreau, "Traveling salesman problems with profits," *Transportation Science*, vol. 39, no. 2, pp. 188–205, 2005.

[34] X. Wang, H. Dai, H. Huang, Y. Liu, G. Chen, and W. Dou, "Robust scheduling for wireless charger networks," in *IEEE INFOCOM*, 2019, pp. 2323–2331.

[35] A. Ahadi, A. Mozafari, and A. Zarei, "Touring a sequence of disjoint polygons: Complexity and extension," *Theoretical Computer Science*, vol. 556, pp. 45–54, 2014.

[36] X. Tan and B. Jiang, "Efficient algorithms for touring a sequence of convex polygons and related problems," in *TAMC*, 2017, pp. 614–627.

[37] H. Zhang and Y. Vorobeychik, "Submodular optimization with routing constraints," in *AAAI*, vol. 16, 2016, pp. 819–826.

[38] M. Ihle, H. Feldwisch-Drentrup, C. A. Teixeira, A. Witon, B. Schelter, J. Timmer, and A. Schulze-Bonhage, "EPILEPSIAE – A European epilepsy database," *Computer Methods and Programs in Biomedicine*, vol. 106, no. 3, pp. 127–138, 2012.

[39] H. Dai, Q. Ma, X. Wu, G. Chen, D. K. Y. Yau, S. Tang, X. Li, and C. Tian, "CHASE: charging and scheduling scheme for stochastic event capture in wireless rechargeable sensor networks," *IEEE Transactions on Mobile Computing*, vol. 19, no. 1, pp. 44–59, 2020.